# Frustratingly Easy Transferability Estimation

Long-Kai Huang\*, Ying Wei<sup>†</sup>, Yu Rong\*, Qiang Yang<sup>‡</sup>, Junzhou Huang\*

#### Abstract

Transferability estimation has been an essential tool in selecting a pre-trained model and the layers of it to transfer, so as to maximize the performance on a target task and prevent negative transfer. Existing estimation algorithms either require intensive training on target tasks or have difficulties in evaluating the transferability between layers. We propose a simple, efficient, and effective transferability measure named TransRate. With single pass through the target data, TransRate measures the transferability as the mutual information between the features of target examples extracted by a pre-trained model and labels of them. We overcome the challenge of efficient mutual information estimation by resorting to coding rate that serves as an effective alternative to entropy. TransRate is theoretically analyzed to be closely related to the performance after transfer learning. Despite its extraordinary simplicity in 10 lines of codes, TransRate performs remarkably well in extensive evaluations on 22 pre-trained models and 16 downstream tasks.

## 1 Introduction

Transfer learning from standard large datasets (e.g., ImageNet) and corresponding pre-trained models (e.g., ResNet-50) has become a de-facto method for real-world deep learning applications where limited annotated data is ready to use. Unfortunately, the performance gain by transfer learning could vary a lot, even with the possibility of negative transfer [1–3]. First, the relatedness of the source task where a pre-trained model is trained on to the target task largely dictates the performance gain. Second, using pre-trained models in different architectures also leads to uneven performance gain even for the same pair of source and target tasks. Figure 1(a) tells that ResNet-50 pre-trained on ImageNet contribute the most to the target task CIFAR-100, compared to the other model architectures. Finally, the optimal layers to transfer vary from pair of tasks to pair. While higher layers encode more semantic patterns that are specific to source tasks [4], lower-layer features are more generic [5]. Especially if a pair of tasks are not sufficiently similar, determining the optimal layers is expected to strike the balance between transferring only lower-layer features (as higher layers specific to a source task may hurt the performance of a target task) and transferring more higher-layer features (as training more higher-layers from scratch requires extensive labeled data). As shown in Figure 1(b), not transferring the five highest layers is preferred for training with full target data, though transferring all but the two highest layers achieves the highest test accuracy with scarce target data. This suggests the following

**Question:** Which pre-trained model (possibly trained on different source tasks in a supervised or unsupervised manner) and which layers of it should be transferred to benefit the target task the most?

This research question drives the design of transferability estimation methods, including computation-intensive [6–9] and computation-efficient ones [10–14]. The pioneering works [6, 9] directly follow the definition of transfer learning to measure the transferability, and thereby require running fine-tuning on a target task with expensive parameter optimization. Though their follow-ups [7, 8] alleviate the need of fine-tuning, their prerequisites still include an encoder pre-trained on the target task. Keeping in mind that

<sup>\*</sup>Tencent AI Lab

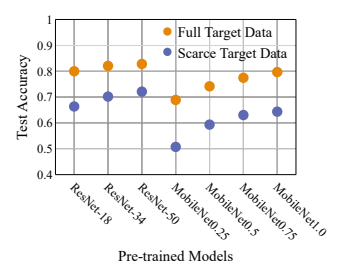
<sup>&</sup>lt;sup>†</sup>Corresponding author; Department of Computer Science, City University of Hong Kong

<sup>&</sup>lt;sup>‡</sup>Hong Kong University of Science and Technology

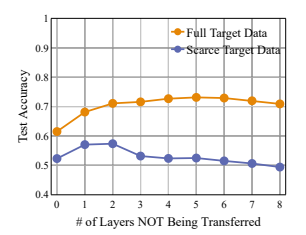
Email: hlongkai@gmail.com, yingwei@cityu.edu.hk, yu.rong@hotmail.com, qyang@cse.ust.hk, jzhuang@uta.edu.

the primary goal of a transferability measure is to select a pre-trained model prior to training on a target task, researchers recently turned towards computation-efficient ways. The transferability is estimated as the negative conditional entropy between the labels of the two tasks in [13] and [12]. Bao et al. [10] and You et al. [14] solved two surrogate optimization problems to estimate the likelihood and marginalized likelihood of labeled target examples, under the assumption that a linear classifier is added on top of the pre-trained model. However, the computation efficiency comes at the price of failing to discriminate the transferability between layers, for both [12, 13] that estimate with labels only and [10, 14] that consider transferring the penultimate layer only.

We are motivated to pursue a "frustratingly easy" transferability measure named TransRate that combines the merits of both computation-intensive and computation-efficient methods. TransRate estimates the mutual information between the features of target examples extracted by a pre-trained model and the labels of them. Though mutual information itself is notoriously challenging to estimate [15], we overcome this obstacle by resorting to the coding rate proposed in [16] inspired from the close connection between rate distortion and entropy in information theory [17]. Such an estimation offers the following advantages: 1) it perfectly



(a) Test accuracy for pre-training ImageNet with different model architectures.



(b) Test accuracy for transferring different layers of the pre-trained ResNet34 model.

Figure 1: Transferring from ImageNet to CIFAR-100. For "Full Target Data", all target data are used, while for "Scarce Target Data", only 50 target samples per class are used in training.

matches our need in computation efficiency, free of either prohibitively exhaustive discretization [18] or neural network training [19]; 2) it is well defined for finite examples from a subspace-like distribution, even if the examples are represented in a high dimensional feature space of a pre-trained model. In a nutshell, TransRate is simple and efficient, as the only computations it requires are (1) making a single forward pass of the model pre-trained on a source task through the target examples to obtain their features at a set of selected layers and (2) calculating the coding rate.

Despite being "frustratingly easy", TransRate enjoys the following benefits that we would highlight.

- Besides selecting a model pre-trained on potentially different tasks in an either supervised or unsupervised way with various model architectures, TrasRate allows to select the layers of the model to transfer.
- TransRate is proved to closely align with the performance after transfer learning, and interpretable in its preference for a pre-trained model that produces complete and compact features.
- TransRate offers surprisingly good performance on evaluation of the transferability between source tasks, model architectures, and layers. We investigate a total of 22 pre-trained models (including supervised, unsupervised, convolutional and graph neural networks), 16 downstream tasks (including classification and regression), and its insensitivity against the number of training examples and classes in a target task.

## 2 Related Works

Re-training or fine-tuning a pre-trained model is a simple yet effective strategy in transfer learning [1]. To improve the performance on a target task and avoid negative transfer, there have been various works on transferability estimation between tasks [6, 10, 11, 7, 12, 8, 13, 9], which we summarize in Table 1. Taskomomy [9] and Task2Vec [6] evaluate the task relatedness by the loss and the Fisher Information Matrix after fully performing fine-tuning of the pre-trained model on the target task, respectively. In RSA [7] and DEPARA [8], the authors proposed to build a similarity graph between examples for each task based on representations by a pre-trained model on this task, and took the graph similarity across tasks as the

Table 1: Summary	of the existing	transferability	measures and ours.

Measures	Free of Training on Target	Free of Assessing Source	Free of Optimization	Applicable to Unsupervised Pre-trained Models	Applicable to Layer Selection
Taskonomy [9] Task2Vec [6] RSA [7] DEPARA [8]	× × ×	× × √	√ × √ √	√ √ √ √	× × √
DS [11] NCE [13]	<b>√</b> ✓	× ×	×	√ ×	×
H-Score [10] LogME [14]	<b>√</b> ✓	√ √	× ×	√ √	××
LEEP [12] TransRate	<b>√</b> ✓	√ √	<b>√</b> ✓	× √	× √

transferability. Despite their general applicability in using unsupervised pre-trained models besides supervised ones and selecting the layer to transfer, their computational costs that are as high as fine-tuning with target labeled data exclude their applications to meet the urgent need of transferability estimation prior to fine-tuning.

This work is more aligned with recent attempts towards computationally efficient transferability measures without training on target data [10–14]. The Earth Mover's Distance between features of the source and the target is used in [11]. Tran et al. [13] proposed the NCE score to estimate the transferability by the negative conditional entropy between labels of a target and a source task. But alas, the source dataset that a pre-trained model has been trained on is oftentimes inaccessible due to memory and privacy issues, disabling the two methods. To bypass the limitations, Bao et al. [10] and You et al. [14] proposed to directly estimate the likelihood and the marginalized likelihood of labeled target examples, respectively, by assuming that a linear classifier is added on top of the pre-trained model. Nguyen et al. [12] proposed the LEEP score, where source labels used in NCE [13] are replaced with soft labels generated by the pre-trained model. Neither of the three, however, is designed for layer selection – H-Score [10] and LogME [14] consider the penultimate layer to be transferred only and LEEP estimating the transferability with labels only fails to differentiate by layers. Our purpose of the proposed TransRate is a simple but effective transferability measure: 1) it is optimization-free with single forward pass, without solving optimization problems as in [10, 14]; 2) besides selecting the source and the architecture of a pre-trained model, it supports layer selection to fill the gap in computationally-efficient measures.

## 3 TransRate

#### 3.1 Notations and Problem Settings

We consider the knowledge transfer from a source task  $T_s$  to a target task  $T_t$  of C-category classification. As widely accepted, only the model that is pre-trained on the source task, instead of source data, is accessible. The pre-trained model, denoted by  $F = f_{L+1} \circ ... \circ (f_2 \circ f_1)$ , consists of an L-layer feature extractor and a 1-layer classifier  $f_{L+1}$ . Here,  $f_l$  is the mapping function at the l-th layer. The target task is represented by n labeled data samples  $\{(x_i, y_i)\}_{i=1}^n$ . Afterwards, we denote the number of layers to be transferred by K ( $K \leq L$ ). These K layers of the model are named as the pre-trained feature extractor  $g = f_K \circ ... \circ (f_2 \circ f_1)$ . The feature of  $x_i$  extracted by g is denoted as  $z_i = g(x_i)$ . Building on the feature extractor, we construct the target model denoted by h to include 1) the same structure as the (K+1)-th to (L)-th layers of the source model and 2) a new classifier  $f_{L+1}^t$  for the target task. We also refer h as the head of the target model.

Following the standard practice of fine-tuning, both the feature extractor g and the head h will be trained on the target task.

We consider the optimal model for the target task as

$$g^*, h^* = \underset{\tilde{g} \in \mathcal{G}, h \in \mathcal{H}}{\operatorname{arg max}} \mathcal{L}(\tilde{g}, h) = \underset{\tilde{g} \in \mathcal{G}, h \in \mathcal{H}}{\operatorname{arg max}} \frac{1}{n} \sum_{i=1}^{n} \log p(y_i | z_i; \tilde{g}, h)$$

subject to  $\tilde{g}^{(0)} = g$ , where  $\mathcal{L}$  denotes the log-likelihood, and  $\mathcal{G}$  and  $\mathcal{H}$  are the spaces of all possible feature extractors and heads, respectively. We define the transferability as the expected log-likelihood of the optimal model  $h^* \circ g^*$  on test samples in the target task:

**Definition 1** (Transferability). The transferability of a pre-trained feature extractor g from a source task  $T_s$  to a target task  $T_t$ , denoted by  $\text{Trf}_{T_s \to T_t}(g)$ , is measured by the expected log-likelihood of the optimal model  $h^* \circ g^*$  on a random test sample (x, y) of  $T_t$ :  $\text{Trf}_{T_s \to T_t}(g) := \mathbb{E}[\log p(y|z; g^*, h^*)]$  where  $z = g^*(x)$ .

This definition of transferability can be used for 1) selection of a pre-trained feature extractor that ranks the highest among a model zoo  $\{g_m\}_{m=1}^M$  for a target task, where the pre-trained models could be in different architectures and trained on different source tasks in a supervised or unsupervised manner, and 2) selection of a layer to transfer among all configurations  $\{g_m^l\}_{l=1}^K$  given a pre-trained model  $g_m$  and a target task.

## 3.2 Computation-Efficient Transferability Estimation

Computing the transferability defined in Definition 1 is as prohibitively expensive as fine-tuning all M pre-trained models or K layer configurations of a pre-trained model to the target task, while the transferability offers benefits only when it can be calculated a priori. To address this shortfall, we propose TransRate, a frustratingly easy measure, to estimate the defined transferability. The transferability characterizes how well the optimal model, composed of the feature extractor  $g^*$  initialized from g and the head  $h^*$ , performs on the target task, where the performance is evaluated by the log-likelihood. However, the optimal model  $h^* \circ g^*$  is inaccessible without optimizing  $\mathcal{L}(\tilde{g},h)$ . For tractability, we follow prior computational-efficient transferability measures [12, 14] to estimate the performance of  $h^* \circ g$  instead. By reasonably assuming that  $h^*$  can extract all the information related to the target task in the pre-trained feature extractor g, we argue that the mutual information between the pre-trained feature extractor g and the target task serves as a strong indicator for the performance of the model  $h^* \circ g$ . Therefore, the proposed TransRate measures this mutual information as,

$$\operatorname{TrR}_{T_s \to T_t}(g) = H(Z) - H(Z|Y), \tag{1}$$

where Y are labels of target examples and Z = g(X) are features of them extracted by the pre-trained feature extractor g. Based on the theory in [20], Proposition 1 shows that TransRate provides an upper bound to the log-likelihood of the model  $h^* \circ g$ . Detailed proofs can be found in Appendix C.

**Proposition 1.** Assume the target task has a uniform label distribution, i.e.  $p(Y = y^c) = \frac{1}{C}$  holds for all c = 1, 2, ..., C. We then have:

$$\operatorname{TrR}_{T_s \to T_t}(g) - H(Y) \gtrsim \mathcal{L}(g, h^*) \gtrsim \operatorname{TrR}_{T_s \to T_t}(g) - H(Y) - H(Z),$$

Computing the TransRate in (1), however, remains a daunting challenge, as the mutual information is notoriously difficult to compute especially for continuous variables in high-dimensional settings [15]. A popular solution for mutual information estimation is to use the histogram method for discretization [18], though it requires an extremely large memory capacity. Even if we divide each dimension of Z into only 10 bins, there will be  $10^d$  bins where d is the dimension of Z that is usually greater than 128. Other estimators include kernel density estimator [21] and k-NN estimator [22, 23]. KDE suffers from singular solutions when the number of examples is smaller than their dimension; the k-NN estimator requiring exhaustive computation of nearest neighbors of all examples may be too computationally expensive if more examples are available. Recent trends in deep neural networks have lead to a proliferation studies of approximating

the mutual information or entropy by a neural network [19, 15, 24] and obtain an high-accuracy estimation by optimizing the neural network. Unfortunately, training neural networks is contrary to our premise of an optimization-free transferability measure.

Fortunately, the rate distortion  $R(Z,\epsilon)$  which defines the minimal number of binary bits to encode Z with an expected decoding error less than  $\epsilon$  serves as an effective alternative to H(Z) [17]. Lastras-Montaño [25] have also shown the connection of rate distortion in neural networks to the log-likelihood. Most crucially, the work of [16] offers an efficient and accurate estimation of  $R(\hat{Z},\epsilon)$  for n finite samples  $\hat{Z} = [z_1, z_2, ..., z_n] \in \mathbb{R}^{d \times n}$  from a subspace-like distribution, even if the samples are in high-dimensional feature representations or from a non-Gaussian distribution. Concretely,

$$R(\hat{Z}, \epsilon) = \frac{1}{2} \log \det(I_d + \frac{d}{n\epsilon^2} \hat{Z} \hat{Z}^\top), \tag{2}$$

where d is the dimension of  $z_i$ , and  $\epsilon$  is the distortion rate. More properties of this rate distortion estimate will be discussed in Appendix C.

Next we investigate the rate distortion estimate  $R(\hat{Z}, \epsilon|Y)$  as an alternative to the second component of TransRate, i.e., H(Z|Y). Define  $Z^c = \{z|Y = y^c\}$  as the random variable for features of the target samples in the c-th class, whose labels are all  $y^c$ . We then have

$$H(Z|Y) = -\int_{z \in Z} \sum_{y \in Y} p(z, y) \log p(z|y) dz = -\int_{z \in Z} \sum_{c=1}^{C} p(z, Y = y^{c}) \log p(z|Y = y^{c}) dz$$

$$= -\int_{z \in Z} \sum_{c=1}^{C} p(Y = y^{c}) p(z|Y = y^{c}) \log p(z|Y = y^{c}) dz$$

$$= \sum_{c=1}^{C} \frac{n_{c}}{n} \int_{z \in Z^{c}} -p(z) \log p(z) dz = \sum_{c=1}^{C} \frac{n_{c}}{n} H(Z^{c}),$$
(3)

where  $n_c$  is the number of training samples in the c-th class. According to (3), it is direct to derive

$$R(\hat{Z}, \epsilon | Y) = \sum_{c=1}^{C} \frac{n_c}{n} R(\hat{Z}^c, \epsilon) = \sum_{c=1}^{C} \frac{n_c}{2n} \log \det(I_d + \frac{d}{n_c \epsilon^2} \hat{Z}^c \hat{Z}^{c \top}), \tag{4}$$

where  $\hat{Z}^c = [z_1^c, z_2^c, ..., z_{n_c}^c] \in \mathbb{R}^{d \times n_c}$  denotes  $n_c$  samples in the c-th class. Combining (2) and (4), we conclude with the TransRate score that we use in practice for transferability estimation:

$$\operatorname{TrR}_{T_s \to T_t}(g, \epsilon) = R(\hat{Z}, \epsilon) - R(\hat{Z}, \epsilon | Y).$$

To avoid confusion, we adopt  $\operatorname{TrR}_{T_s \to T_t}(g)$  and  $\operatorname{TrR}_{T_s \to T_t}(g, \epsilon)$  to denote the ideal and the working TransRate, respectively. The distortion rate  $\epsilon$  calibrates how close  $R(\hat{Z}, \epsilon)$  is to H(Z) – a smaller  $\epsilon$  leads to a more precise estimation. Fortunately,  $\epsilon$  has minimal influence to the performance of  $\operatorname{TrR}_{T_s \to T_t}(g, \epsilon)$ . For a sufficiently small  $\epsilon$ , the value of  $R(\hat{Z}, \epsilon)$  is dominated by  $\log \det(\frac{d}{n\epsilon^2}\hat{Z}\hat{Z})$  and similar for  $R(\hat{Z}, \epsilon|Y)$ . Though scaling  $\epsilon$  by a positive constant  $\alpha$  approximately increases both values of  $R(\hat{Z}, \epsilon)$  and  $R(\hat{Z}_c, \epsilon)$  by  $-2\log(\alpha)$ ,  $\operatorname{TrR}_{T_s \to T_t}(g, \epsilon)$  that subtracts  $R(\hat{Z}_c, \epsilon|Y)$  from  $R(\hat{Z}, \epsilon)$  cancels out such increase. Besides, we empirically validate that the performance of  $\operatorname{TrR}_{T_s \to T_t}(g, \epsilon)$  is almost insensitive to the value of  $\epsilon$  in Appendix B.

Completeness and Compactness We argue that TransRate favors those pre-trained models that produce both complete and compact features. (1) Completeness:  $R(\hat{Z}, \epsilon)$  as the first term of  $\text{TrR}_{T_s \to T_t}(g, \epsilon)$  evaluates whether the features  $\hat{Z}$  by the pre-trained feature extractor g include sufficient information for solving the target task – features between different classes of examples are expected to be as diverse as possible.  $\hat{Z}$  in Figure 2(a) is more diverse than that in Figure 2(c), evidenced by a larger value of  $R(\hat{Z}, 0.1)$ . (2) Compactness: The second term, i.e.,  $-R(\hat{Z}, \epsilon|Y)$ , assesses whether the features  $\hat{Z}^c$  for each c-th class are compact enough

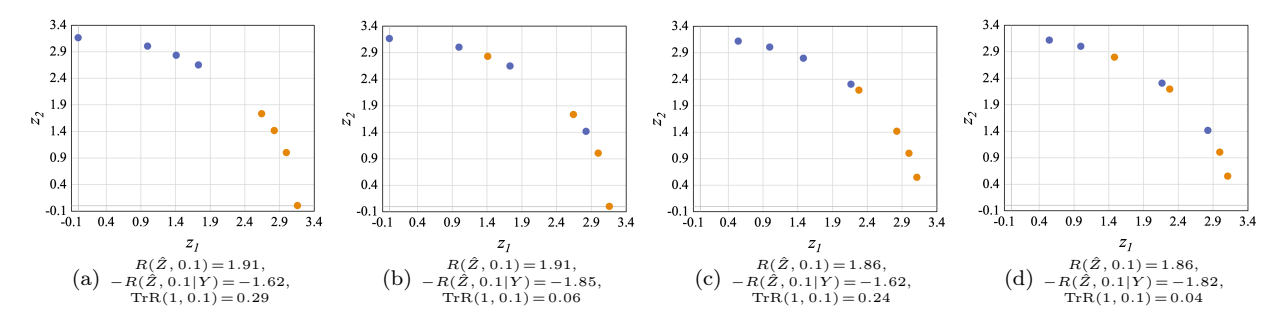


Figure 2: Toy examples illustrating the effectiveness of the TransRate. The horizontal and vertical axes represent the two dimensions of features  $\hat{Z}$ . There are two classes in Y, pictorially illustrated with two colors.

for good generalization capacity. Each of the two classes spans a wider range in Figure 2(b) than that in Figure 2(a), so that the value of  $-R(\hat{Z}, 0.1|Y)$  (-1.85) is smaller.

Furthermore, there is theoretical evidence to strengthen the argument above. Consider a binary classification problem with  $\hat{Z} = [\hat{Z}^1, \hat{Z}^2] \in \mathbb{R}^{d \times n}$ , where both  $\hat{Z}^1$  and  $\hat{Z}^2$  have n d-dim examples. By defining  $\alpha = d/(n\epsilon^2)$ , we have  $\mathrm{TrR}_{T_s \to T_t}(g, \epsilon) = \frac{1}{2} \log \det\{(I_{n/2} + \alpha(\hat{Z}^1)^\top \hat{Z}^1 + \alpha(\hat{Z}^2)^\top \hat{Z}^2) + \alpha^2[(\hat{Z}^1)^\top \hat{Z}^1(\hat{Z}^2)^\top \hat{Z}^2 - (\hat{Z}^1)^\top \hat{Z}^2(\hat{Z}^2)^\top \hat{Z}^1]\} - B$  where  $B = \frac{1}{2}(R(Z_1, \epsilon) + R(Z_2, \epsilon))$ . We assume  $(\hat{Z}^1)^\top \hat{Z}^1$  and  $(\hat{Z}^2)^\top \hat{Z}^2$  to be fixed, so that TransRate maintaining the compactness within each class, where B becomes a constant, and hinging on the completeness only maximizes at  $(\hat{Z}^1)^\top \hat{Z}^2 = 0$  and minimizes at  $\hat{Z}_1 = \hat{Z}_2$ . That is, TransRate favors the diversity between different classes, while penalizes if the overlap between classes is high. More detailed proof can be found in Appendix C.

## 4 Experiments

In this section, we evaluate the correlation between predicted transferability by TransRate and the transfer learning performance in various settings and for different tasks. Due to page limit, experiments covering more settings and the wall-clock time comparison are available in Appendix B.

#### 4.1 Implementation Details

We consider fine-tuning a pre-trained model from a source dataset to the target task without access to any source data. For fine-tuning of the target task, the feature extractor is initialized by the pre-trained model. Then the feature extractor together with a randomly initialized head is optimized by running SGD on a cross-entropy loss for 100-epoch with the batch size being 10. The learning rate (from 0.0001 to 0.1) and weight decays (from 1E-6 to 1E-4) are obtained via grid search based on the best average transfer performance on a validation set over 10 runs of experiments.

Before performing fine-tuning on the target task, we calculate TransRate and the other transferability measures by baselines on training examples of the target task. To compute the proposed TransRate score, we first run a single forward pass of the pre-trained model through all target examples to extract their features  $\hat{Z}$ . Second, we compute the TransRate score as  $R(\hat{Z}, \epsilon) - R(\hat{Z}, \epsilon|Y)$ . In the experiments, we set  $\epsilon^2 = 0.1$  by default. The sensitivity of TransRate to the value of  $\epsilon^2$  is studied in Appendix B. As the scale of features extracted by different feature extractors may vary a lot, we normalize the features to have unit norm before calculating the coding rate.

We adopt LEEP [12], NCE [13], Label-Feature Correlation (LFC) [26], H-Score [10] and LogME [14] as the baseline methods. For a fair comparison, we assume no data from source tasks is available. In this scenario, the NCE score, defined by  $-H(Y|Y_S)$  where  $Y_S$  is the labels from the source task, cannot be computed following the procedure described in its original paper. Instead, we follow [12] to replace  $Y_S$  with the softmax label generated by the classifer of the pre-trained model. Another setting for a fair comparison is that only one single forward pass through the target examples is allowed for computational efficiency. In this case, the optimal target features for transferability estimation in [10] are not available. As suggested by [10], we

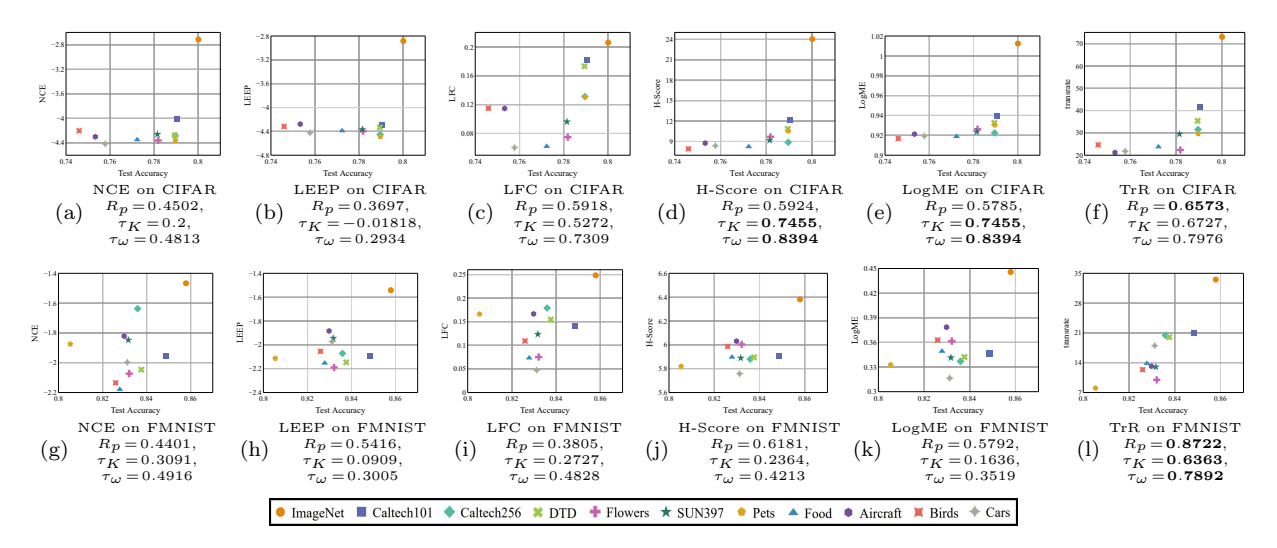


Figure 3: Transferability estimation on transferring ResNet-18 pre-trained on 11 different source datasets to CIFAR-100 and Fashion-MNIST.

calculate its estimate using the H-Score by pre-trained features and skip the computation of H-Score based on the optimal target features.

To measure the performance of TransRate and five baseline methods in estimating the transfer learning performance, we follow [12, 13] to compute the Pearson correlation coefficient between the score and the average accuracy of the fine-tuned model on testing samples of the target set. The Kendall's  $\tau$  [27] and its variant, weighted  $\tau$ , are also adopted as performance metrics. For brief, we denote the Pearson correlation coefficient, Kendall's  $\tau$  and weighted  $\tau$  by  $R_p$ ,  $\tau_K$ , and  $\tau_\omega$ , respectively.

#### 4.2 TransRate as a Criterion for Source Selection

One of the most important applications of TransRate is source model selection for a target task. In the experiments, we evaluate the performance of TransRate and other baseline measures for selection of a pre-trained model from 11 source datasets to a specific target task. The source datasets are ImageNet [28] and 10 image datasets from [29], including Caltech-101, Caltech-256, DTD, Flowers, SUN397, Pets, Food, Aircraft, Birds and Cars. For each source dataset, we pre-train a ResNet-18 [30], freeze it and discard the source data during fine-tuning the target task. CIFAR-100 [31] and Fashion-MNIST (FMNIST) [32] are adopted as the target tasks. The details of these datasets and their pre-trained models are available in Appendix A; experiments on more target tasks are available in Appendix B.

We present the results in Figure 3. LFC, H-Score, LogME and TransRate all correctly predict the top-3 source models for CIFAR-100. TransRate achieves the best  $R_p$ , which means that TransRate is more linearly correlated to the transfer performance than the baselines. TransRate also achieves a competitive  $\tau_K$  and  $\tau_\omega$ , which is just slightly inferior to those of H-Score and LogME. As for FMNIST, TransRate correctly predicts the top-4 source models, while all the other baselines fail to accurately predict the rank of the Caltech-101 model, which comes the second among all the models. TransRate outperforms the baselines by a large margin in all correlation coefficients. These results demonstrate that TransRate can serve as a practical criterion for source selection in transfer learning.

#### 4.3 TransRate as a Criterion for Layer Selection

As introduced in Section 1, transferring different layers of the pre-trained model results in different accuracies; that is, the optimal layers to transfer are task-specific. To study the correlation between all transferability measures and the performance of transferring different layers, we conduct experiments on transferring the first layer to the K-th layer only. In this experiment, we consider transferring a ResNet-20 model pre-trained

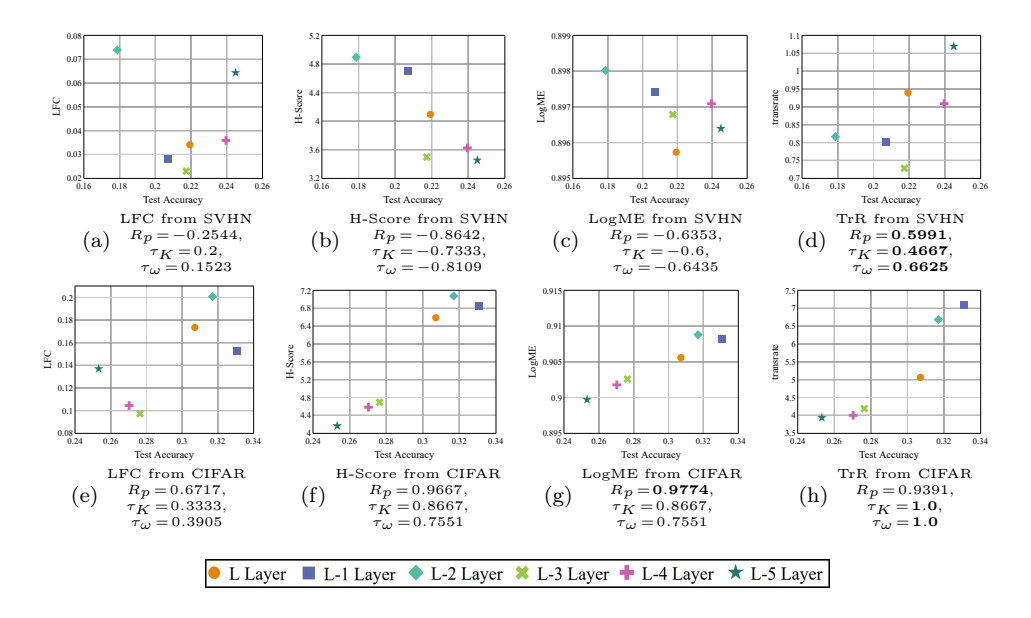


Figure 4: Transferability estimation on transferring different layers of ResNet-20 pre-trained on CIFAR-10 and SVHN to CIFAR-100.

on CIFAR-10 or SVHN to CIFAR-100. The candidate values of K for ResNet-20 are  $\{9,11,13,15,17,19\}$ . After determining the layers to transfer, these selected layers are initialized by the pre-trained model and the remaining layers are trained from scratch. Specifically, we simulate a scenario of scarce training data in the target tasks by involving only 50 training examples for each class in CIFAR-100. As the data is scarce, the model is optimized within only 50 epochs of SGD. NCE and LEEP are excluded in this experiment as they are not applicable to layer selection. For TransRate and other baselines, the transferability is estimated by the features extracted by the first K-th layer. Note that when K is not the last layer, we will apply the average pooling function on the features, which is used by the original ResNet-20 in the last layer. As a result, different layers will have different dimensions, while the value of TransRate is affected by the dimension of features. To enable comparison between TransRate computed on features with different dimensions, we normalize TransRate by multiplying a factor  $\sqrt{d/512}$ , where 512 is the dimension of the last layer of ResNet-20. More details about the experimental settings are available in Appendix A.

From the results in Figure 4, we observe that TransRate is the only method that correctly predicts the layer with the highest performance in both experiments. In the experiment transferring different layers of the pre-trained model from SVHN, TransRate achieves the highest correlation coefficients  $R_p$ ,  $\tau_K$ ,  $\tau_\omega$ . The baselines even have negative coefficients, which means that their predictions are inverse to the correct ranking. In the experiment transferring from CIFAR-10, TransRate correctly predicts the whole rank of the transfer performance after different layers are transferred and also achieves a high  $R_p$ . Though H-Score and LogME achieve even better  $R_p$  in this experiment, they both fail to predict the best layer to be transferred. Both experiments demonstrate the superiority of TransRate in selecting the best layer for transfer. More experiments of layer selection with different source datasets, models, and target datasets are available in Appendix B.

#### 4.4 TransRate as a Criterion for Pre-trained Model Selection

Another important application of transferability measures is the selection of pre-trained models in different architectures. In practice, various pre-trained models are available for public large datasets. For example, PyTorch provides more than 20 pre-trained neural networks for ImageNet. To maximize the transfer performance from such a dataset, it is necessary to estimate the transferability of various model candidates and select the one with the maximal score to transfer. In this experiment, we study the correlation between

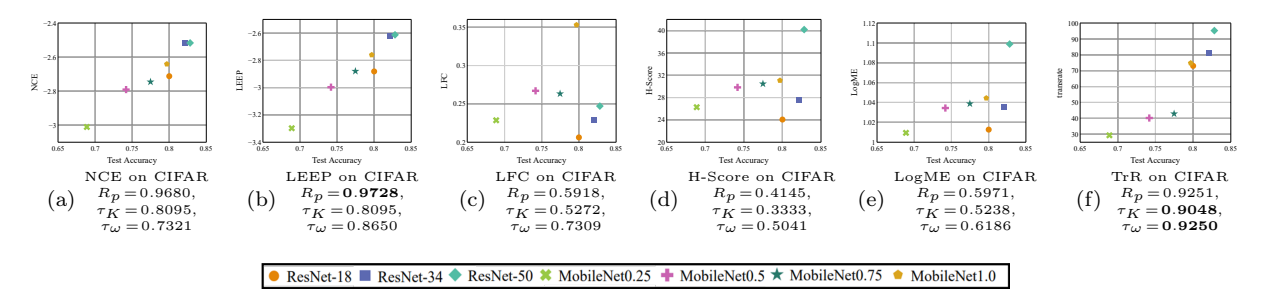


Figure 5: Result on transferring models with different architectures from ImageNet to CIFAR-100.

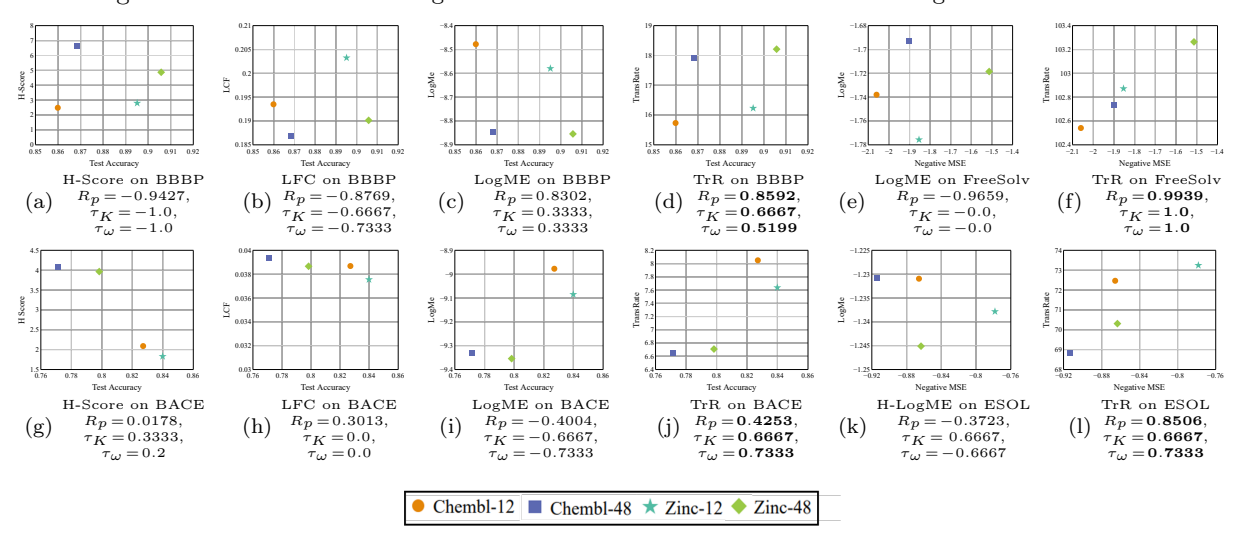


Figure 6: Result on transfering GNNs pre-trained on molecules sampled from different datasets to molecule property prediction tasks.

each transferability measure and the transfer accuracy after transferring seven kinds of pre-trained models on ImageNet to CIFAR-100. The seven types of pre-trained models include ResNet18 [30], ResNet34, ResNet50, MobileNet0.25, MobileNet0.5, MobileNet0.75, MobileNet1.0 [33].

From the results in Figure 5, we observe that TransRate in general has a significant linear correlation to the transfer accuracy, though it slightly underestimates the accuracy of ResNet-18 or overestimates MobileNet1.0. Also, TransRate achieves the best ranking prediction as evidenced by the larget  $\tau_K$  and  $\tau_{\omega}$ . Though the predictions of LEEP and NCE achieve the best  $R_p$ , they underestimate ResNet-18, ranking it incorrectly. This also explains why they obtain lower  $\tau_K$  and  $\tau_{\omega}$  than TransRate. As for LFC, H-Score and LogME, their performances are not as competitive as NCE, LEEP and TransRate.

# 4.5 Estimation of Unsupervised Pre-trained Models to Classification and Regression Tasks

In this part, we evaluate the effectiveness of TransRate and the baselines on estimating transferability from different unsuperivsed pre-trained models. To do this, we adopt the unsupervised GNN model, GROVER [34], with two different sizes of hidden units. The smaller model contains about 12 million parameters while the larger one has about 48 million parameters. Each of the two models is pre-trained on two unlabeled molecules datasets. The first one has 2 million molecules collected from ChemBL [35] and MoleculeNet [36]; the second one contains 11 million molecules sampled from ZINC15 [37] and ChemBL. In total, we have 4 different pre-trained models, denoted by ChemBL-12, ChemBL-48, Zinc-12, Zinc-48. We consider four target tasks that predict the molecular ADMET properties, including BBBP [38], BACE [39], Esol [40], FreeSolv [41].

The BBBP and BACE are classification tasks, while Esol and FreeSolv are regression tasks. More details about the settings of the pre-trained GNN models and the datasets are available in Appendix A.

From the results displayed in Figure 6, we observe that in all four experiments, TransRate achieves the best performance regarding all 3 coefficients. To be specific, TransRate correctly predicts the best model in all experiments except the one on BACE, while the competitors all fail to predict the best model. These results demonstrate the wide applicability as well as the effectiveness of the proposed TransRate in transferring from unsupervised pre-trained models and to regression target tasks.

#### Sample Size Sensitivity Analysis 4.6

The performance of a transfer learning algorithm is widely accepted to be empirically correlated with the number of training samples [42]. The generalization theory also speaks for the dependency of the transferability estimation on the number of samples involved in estimation. Both highlight the pressing necessity of developing a robust transferability estimation algorithm that is not sensitive to the change of the training sample size. In this experiment, we estimate the sensitivity of TransRate and the baseline methods with regard to the number of training samples in the target task. We adopt the same experiment settings as in Section 4.2, except that the number of samples available for each class varies from 50 to 500.

From the results in Figure 7, we observe that the performance of TransRate does not significantly drop with the decrease of the sample size, while the performances of other methods generally decrease. This indicates the superiority of TransRate

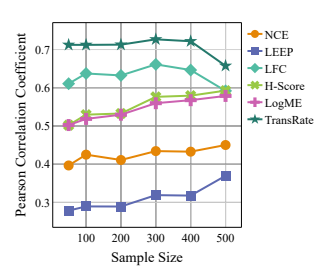


Figure 7: Influence of the sample size of target datasets to the performance of a transferability measure. The performance is measured by the correlation coefficient when fine-tuning the pre-trained ResNet-18 from 11 different source datasets to CIFAR-100.

in transferability estimation even when only a small amount of training samples are available.

#### Conclusion and Limitations 5

In this paper, we propose a computation-efficient transferability measure named TransRate that flexibly supports estimation for transferring both holistic and partial layers of a pre-trained model. TransRate estimates the mutual information between the features extracted by a pre-trained model and labels with the coding rate. The theoretic and empirical studies both demonstrate that TransRate has a strong correlation to the transfer learning performance, making it a qualified transferability measure for source dataset, model, and layer selection. So far we only consider the transfer strategy of fine-tuning, while in the future we would improve it to also take into account different transfer strategies, e.g., knowledge distillation.

#### References

- [1] Sinno Jialin Pan and Qiang Yang. A survey on transfer learning. IEEE Transactions on knowledge and data engineering, 22(10):1345–1359, 2009.
- [2] Zirui Wang, Zihang Dai, Barnabás Póczos, and Jaime Carbonell. Characterizing and avoiding negative transfer. In CVPR, pages 11293–11302, 2019.
- [3] Wen Zhang, Lingfei Deng, and Dongrui Wu. Overcoming negative transfer: A survey. arXiv preprint arXiv:2009.00909, 2020.
- [4] Xu Yang, Hanwang Zhang, and Jianfei Cai. Deconfounded image captioning: A causal retrospect. arXiv  $preprint\ arXiv:2003.03923,\ 2020.$

- [5] Jason Yosinski, Jeff Clune, Yoshua Bengio, and Hod Lipson. How transferable are features in deep neural networks? In *NeurIPS*, pages 3320–3328, 2014.
- [6] Alessandro Achille, Michael Lam, Rahul Tewari, Avinash Ravichandran, Subhransu Maji, Charless C Fowlkes, Stefano Soatto, and Pietro Perona. Task2vec: Task embedding for meta-learning. In ICCV, pages 6430–6439, 2019.
- [7] Kshitij Dwivedi and Gemma Roig. Representation similarity analysis for efficient task taxonomy & transfer learning. In CVPR, pages 12387–12396, 2019.
- [8] Jie Song, Yixin Chen, Jingwen Ye, Xinchao Wang, Chengchao Shen, Feng Mao, and Mingli Song. Depara: Deep attribution graph for deep knowledge transferability. In *CVPR*, pages 3922–3930, 2020.
- [9] Amir R Zamir, Alexander Sax, William Shen, Leonidas J Guibas, Jitendra Malik, and Silvio Savarese. Taskonomy: Disentangling task transfer learning. In *CVPR*, pages 3712–3722, 2018.
- [10] Yajie Bao, Yang Li, Shao-Lun Huang, Lin Zhang, Lizhong Zheng, Amir Zamir, and Leonidas Guibas. An information-theoretic approach to transferability in task transfer learning. In *ICIP*, pages 2309–2313, 2019.
- [11] Yin Cui, Yang Song, Chen Sun, Andrew Howard, and Serge Belongie. Large scale fine-grained categorization and domain-specific transfer learning. In *CVPR*, pages 4109–4118, 2018.
- [12] Cuong V Nguyen, Tal Hassner, Cedric Archambeau, and Matthias Seeger. Leep: A new measure to evaluate transferability of learned representations. *ICML*, 2020.
- [13] Anh T Tran, Cuong V Nguyen, and Tal Hassner. Transferability and hardness of supervised classification tasks. In *ICCV*, pages 1395–1405, 2019.
- [14] Kaichao You, Yong Liu, Mingsheng Long, and Jianmin Wang. Logme: Practical assessment of pre-trained models for transfer learning. arXiv preprint arXiv:2102.11005, 2021.
- [15] R Devon Hjelm, Alex Fedorov, Samuel Lavoie-Marchildon, Karan Grewal, Phil Bachman, Adam Trischler, and Yoshua Bengio. Learning deep representations by mutual information estimation and maximization. In ICLR, 2019.
- [16] Yi Ma, Harm Derksen, Wei Hong, and John Wright. Segmentation of multivariate mixed data via lossy data coding and compression. *IEEE transactions on pattern analysis and machine intelligence*, 29(9): 1546–1562, 2007.
- [17] Thomas M Cover. Elements of information theory. John Wiley & Sons, 1999.
- [18] Naftali Tishby and Noga Zaslavsky. Deep learning and the information bottleneck principle. In 2015 IEEE Information Theory Workshop (ITW), pages 1–5. IEEE, 2015.
- [19] Mohamed Ishmael Belghazi, Aristide Baratin, Sai Rajeshwar, Sherjil Ozair, Yoshua Bengio, Aaron Courville, and Devon Hjelm. Mutual information neural estimation. In *ICML*, pages 531–540, 2018.
- [20] Zhenyue Qin, Dongwoo Kim, and Tom Gedeon. Rethinking softmax with cross-entropy: Neural network classifier as mutual information estimator. arXiv preprint arXiv:1911.10688, 2019.
- [21] Young-Il Moon, Balaji Rajagopalan, and Upmanu Lall. Estimation of mutual information using kernel density estimators. *Physical Review E*, 52(3):2318, 1995.
- [22] Jan Beirlant, Edward J Dudewicz, László Györfi, and Edward C Van der Meulen. Nonparametric entropy estimation: An overview. *International Journal of Mathematical and Statistical Sciences*, 6(1):17–39, 1997.

- [23] Alexander Kraskov, Harald Stögbauer, and Peter Grassberger. Estimating mutual information. *Physical review E*, 69(6):066138, 2004.
- [24] Yuval Shalev, Amichai Painsky, and Irad Ben-Gal. Neural joint entropy estimation. arXiv preprint arXiv:2012.11197, 2020.
- [25] Luis A Lastras-Montaño. Information theoretic lower bounds on negative log likelihood. In ICLR, 2018.
- [26] Aditya Deshpande, Alessandro Achille, Avinash Ravichandran, Hao Li, Luca Zancato, Charless Fowlkes, Rahul Bhotika, Stefano Soatto, and Pietro Perona. A linearized framework and a new benchmark for model selection for fine-tuning. arXiv preprint arXiv:2102.00084, 2021.
- [27] Maurice G Kendall. A new measure of rank correlation. Biometrika, 30(1/2):81-93, 1938.
- [28] Olga Russakovsky, Jia Deng, Hao Su, Jonathan Krause, Sanjeev Satheesh, Sean Ma, Zhiheng Huang, Andrej Karpathy, Aditya Khosla, Michael Bernstein, et al. Imagenet large scale visual recognition challenge. *International journal of computer vision*, 115(3):211–252, 2015.
- [29] Hadi Salman, Andrew Ilyas, Logan Engstrom, Ashish Kapoor, and Aleksander Madry. Do adversarially robust imagenet models transfer better? arXiv preprint arXiv:2007.08489, 2020.
- [30] Kaiming He, Xiangyu Zhang, Shaoqing Ren, and Jian Sun. Deep residual learning for image recognition. In CVPR, pages 770–778, 2016.
- [31] Alex Krizhevsky, Geoffrey Hinton, et al. Learning multiple layers of features from tiny images. 2009.
- [32] Han Xiao, Kashif Rasul, and Roland Vollgraf. Fashion-mnist: a novel image dataset for benchmarking machine learning algorithms. arXiv preprint arXiv:1708.07747, 2017.
- [33] Mark Sandler, Andrew Howard, Menglong Zhu, Andrey Zhmoginov, and Liang-Chieh Chen. Mobilenetv2: Inverted residuals and linear bottlenecks. In *CVPR*, pages 4510–4520, 2018.
- [34] Yu Rong, Yatao Bian, Tingyang Xu, Weiyang Xie, Ying Wei, Wenbing Huang, and Junzhou Huang. Self-supervised graph transformer on large-scale molecular data. *Advances in Neural Information Processing Systems*, 33, 2020.
- [35] Anna Gaulton, Louisa J Bellis, A Patricia Bento, Jon Chambers, Mark Davies, Anne Hersey, Yvonne Light, Shaun McGlinchey, David Michalovich, Bissan Al-Lazikani, et al. Chembl: a large-scale bioactivity database for drug discovery. *Nucleic acids research*, 40(D1):D1100–D1107, 2012.
- [36] Zhenqin Wu, Bharath Ramsundar, Evan N Feinberg, Joseph Gomes, Caleb Geniesse, Aneesh S Pappu, Karl Leswing, and Vijay Pande. Moleculenet: a benchmark for molecular machine learning. *Chemical science*, 9(2):513–530, 2018.
- [37] Teague Sterling and John J Irwin. Zinc 15-ligand discovery for everyone. *Journal of chemical information and modeling*, 55(11):2324-2337, 2015.
- [38] Ines Filipa Martins, Ana L Teixeira, Luis Pinheiro, and Andre O Falcao. A bayesian approach to in silico blood-brain barrier penetration modeling. *Journal of chemical information and modeling*, 52(6): 1686–1697, 2012.
- [39] Govindan Subramanian, Bharath Ramsundar, Vijay Pande, and Rajiah Aldrin Denny. Computational modeling of  $\beta$ -secretase 1 (bace-1) inhibitors using ligand based approaches. *Journal of chemical information and modeling*, 56(10):1936–1949, 2016.
- [40] John S Delaney. Esol: estimating aqueous solubility directly from molecular structure. *Journal of chemical information and computer sciences*, 44(3):1000–1005, 2004.

- [41] David L Mobley and J Peter Guthrie. Freesolv: a database of experimental and calculated hydration free energies, with input files. *Journal of computer-aided molecular design*, 28(7):711–720, 2014.
- [42] Wataru Kumagai. Learning bound for parameter transfer learning. NIPS, 2016.
- [43] Subhransu Maji, Esa Rahtu, Juho Kannala, Matthew Blaschko, and Andrea Vedaldi. Fine-grained visual classification of aircraft. arXiv preprint arXiv:1306.5151, 2013.
- [44] Thomas Berg, Jiongxin Liu, Seung Woo Lee, Michelle L Alexander, David W Jacobs, and Peter N Belhumeur. Birdsnap: Large-scale fine-grained visual categorization of birds. In *Proceedings of the IEEE Conference on Computer Vision and Pattern Recognition*, pages 2011–2018, 2014.
- [45] Li Fei-Fei, Rob Fergus, and Pietro Perona. Learning generative visual models from few training examples: An incremental bayesian approach tested on 101 object categories. In 2004 conference on computer vision and pattern recognition workshop, pages 178–178. IEEE, 2004.
- [46] Gregory Griffin, Alex Holub, and Pietro Perona. Caltech-256 object category dataset. 2007.
- [47] Jonathan Krause, Jia Deng, Michael Stark, and Li Fei-Fei. Collecting a large-scale dataset of fine-grained cars. 2013.
- [48] Mircea Cimpoi, Subhransu Maji, Iasonas Kokkinos, Sammy Mohamed, and Andrea Vedaldi. Describing textures in the wild. In *Proceedings of the IEEE Conference on Computer Vision and Pattern Recognition*, pages 3606–3613, 2014.
- [49] Maria-Elena Nilsback and Andrew Zisserman. Automated flower classification over a large number of classes. In 2008 Sixth Indian Conference on Computer Vision, Graphics & Image Processing, pages 722–729. IEEE, 2008.
- [50] Lukas Bossard, Matthieu Guillaumin, and Luc Van Gool. Food-101-mining discriminative components with random forests. In European conference on computer vision, pages 446-461. Springer, 2014.
- [51] Omkar M Parkhi, Andrea Vedaldi, Andrew Zisserman, and CV Jawahar. Cats and dogs. In 2012 IEEE conference on computer vision and pattern recognition, pages 3498–3505. IEEE, 2012.
- [52] Jianxiong Xiao, James Hays, Krista A Ehinger, Aude Oliva, and Antonio Torralba. Sun database: Large-scale scene recognition from abbey to zoo. In 2010 IEEE computer society conference on computer vision and pattern recognition, pages 3485–3492. IEEE, 2010.
- [53] David Barber Felix Agakov. The im algorithm: a variational approach to information maximization. NeurIPS, 16:201, 2004.
- [54] Yaodong Yu, Kwan Ho Ryan Chan, Chong You, Chaobing Song, and Yi Ma. Learning diverse and discriminative representations via the principle of maximal coding rate reduction. *NeurIPS*, 33, 2020.

## A Omitted Experiment Details in Section 4

## A.1 Image Datasets Description

**Aircraft** [43] The dataset consists of 10,000 aircraft images in 100 classes, with 66/34 or 67/33 training/testing images per class.

**Birdsnap** [44] The dataset has 49,829 images of 500 species of North American Birds. It is divided into a training set with 32,677 images and a testing set with 8,171 images.

Caltech-101 [45] The dataset contains 9,146 images from 101 object categories. The number of images in each category is between 40 and 800. Following [29], we sample 30 images per category as a training set and use the rest of images as a testing test.

Caltech-256 [46] The dataset is an extension of Caltech 101. It contains 30,607 images spanning 257 categories. Each category has 80 to 800 images. We sample 60 images per category for training and use the rest of images for testing.

Cars [47] The dataset consists of 16,185 images of 196 classes of cars. It is divided into a training set with 8,144 images and a testing set with 8,041 images.

CIFAR-10 [31] The dataset contains 60,000 color images in 10 classes, with each image in the size of  $32 \times 32$ . Each class has 5,000 training samples and 1,000 testing samples.

CIFAR-100 [31] The dataset is the same as CIFAR-10 except that it has 100 classes each of which contains 500 training images and 100 testing images.

**DTD** [48] The dataset consists of 5,640 textural images with sizes ranging between  $300 \times 300$  and  $600 \times 600$ . There are a total of 47 categories, with 80 training and 40 testing images in each category.

**Fashion MNIST** [32] The dataset involves 70,000 grayscale images from 10 classes with the size of each image as  $28 \times 28$ . Each class has 6,000 training samples and 1,000 testing samples.

**Flowers** [49] The dataset consists of 102 categories of flowers that are common in the United Kindom. Each category contains between 40 and 258 images. We sample 20 images per category to construct the training set and use the rest of 6,149 images as the testing set.

**Food** [50] The dataset contains 101,000 images organized by 101 types of food. Each type of food contains 750 training images and 250 testing images.

**Pets** [51] The dataset contains 7,049 images of pets belonging to 47 species. The training set contains 3,680 images and the testing set has 3,669 images.

**SUN397** [52] This dataset has 397 classes, each having 100 scenery pictures. For each class, there are 50 training samples and 50 testing samples.

#### A.2 Molecule Datasets Description

**BBBP** [38] The dataset contains 2,039 compounds with binary labels of blood-brain barriers penetration. In the dataset, 1560 compounds are positive and 479 compounds are negative.

**BACE** [39] The dataset involves 1,513 recording compounds which could act as the inhibitors of human  $\beta$ -secretase 1 (BACE-1). 691 samples are positive and the rest 824 samples are negative.

**Esol** [40] The dataset documents the water solubility (log solubility in mols per litre) for 1,128 small molecules.

**Freesolv** [41] The dataset contains 642 records of the hydration free energy of small molecules in water from both experiments and alchemical free energy calculations.

Note that on both BBBP and BACE we perform binary classification by training with a binary cross-entropy loss. Yet the regression tasks on Esol and Freesolv datasets are trained by an MSE loss. For all four datasets, we random split 80% samples for training and 20% samples for testing.

#### A.3 Pre-trained Models

In the experiments, all models except GROVER used in Sec. 4.5 follow the standard architectures in PyTorch's torchvision. For those models pre-trained on ImageNet, we directly download them from PyTorch's torchvision.

For those models pre-trained on other source datasets, we pre-train them with the hyperparameters obtained via grid search to guarantee the best performance. For GROVER [34], we run the released codes on two large-scale unlabelled molecule datasets provided by the authors, and obtain a total of 4 pre-trained models as mentioned in Sec 4.5.

## A.4 Details about the Layer Selection Experiments in Section 4.3

In the layer selection experiments, we transfer the first K layers from the pre-trained model and train the remaining layers from scratch. Notice that an average pooling function is applied to aggregate the outputs from different channels in the last layer of ResNet, which reduces the dimension of features. Inspired by this, we also apply an average pooling on the output of the K-th layer to reduce the feature dimension when we compute the score of TransRate, even if K is not the last layer in layer selection. Besides the experiments on ResNet-20, we also conduct layer selection on ResNet-18 and ResNet-34 and present the results in Appendix B.2. The details of candidate layers and the feature dimensions are summarized in Table 2.

Table 2: '	The configurations of	f layer	select	ion fo	r three	e mod	el arcl	nitectu	ires.
ResNet-20	Candidate Layers:	19	17	15	13	11	9		
	Feature Dimension:	64	64	64	32	32	32		
ResNet-18	Candidate Layers: Feature Dimension:	17 512	15 512	13 256	11 256				
ResNet-34	Candidate Layers: Feature Dimension:	33 512	30 512	$\frac{27}{512}$	$\frac{25}{256}$	$\frac{23}{256}$	21 256	19 256	17 256

A.5 Details about Applying TransRate on Regression Tasks

When estimating TransRate on regression target tasks, the label (or target value)  $y_i$  is not discrete so that we cannot directly compute  $R(\hat{Z}, \epsilon|Y)$  in TransRate. The key insight behind TransRate for classification is to estimate the overlap between the features of samples from different classes. Similarly, the transferability in a regression task can be estimated by the extent of the overlap between the features of samples with different target values. To realize this, we rank all n target values  $\{y_i\}_{i=1}^n$  and divide them evenly into 10 ranges. For samples in each range, we compute  $R(\hat{Z}^c, \epsilon)$  where  $\hat{Z}^c$  is the feature matrix of samples in the c-th range. Finally, we calculate  $R(\hat{Z}, \epsilon|Y) = \sum_{c=1}^{C} R(\hat{Z}^c, \epsilon)$  and subtract  $R(\hat{Z}, \epsilon|Y)$  from  $R(\hat{Z}, \epsilon)$  to obtain the resulting TransRate.

#### A.6 Source Codes of TransRate

We implement the TransRate by Python. The codes are as follows:

```
Import Numpy as np
```

```
def coding_rate(Z, eps=0.1):
    n, d = Z.shape
    (_, rate) = np.linalg.slogdet((np.eye(d) + d / (n * eps) * Z @ Z.transpose()))
    return 0.5 * rate

def transrate(feat, y, eps=0.1):
    RZ = coding_rate(Z, eps)
    RZY = 0.
    K = int(y.max() + 1)
    for i in range(K):
        RZY += coding_rate(Z[(y == i).flatten()], eps)
    return RZ - RZY / K
```

Here, we observe that TransRate can be implemented by 9 lines of codes, which demonstrates its simplicity. It takes the features  $\hat{Z}$  ("feat" in the codes) and the labels Y ("y" in the codes) as input, calls the function "coding—rate" to calculate the coding rate of  $R(\hat{Z}, \epsilon)$  and  $R(\hat{Z}, \epsilon|Y)$ , and finally returns the TransRate.

## B Extra Experiments

## **B.1** Extra Experiments on Source Selection

In Table 3, we summarize the results of source selection that we have presented in Section 4.2 and meanwhile include the results of source selection for 9 more target datasets. Since the 11 source datasets include the 9 new target datasets, we remove the model that is pre-trained on the target dataset and consider only the 10 models that are pre-trained on the remaining source datasets. For all target datasets, we use the whole training set for fine-tuning and for transferability estimation.

From Table 3, we observe that TransRate achieves 21/33 best performances and 10/33 second best performances, which indicates the superiority of TransRate across the spectrum of different target datasets. Even for the most competitive baseline H-Score, it only achieves 60% of TransRate with 12/33 best performances. LogME has a similar performance to H-Score, but a little bit worse. As for NCE, LEEP, and LFC, their performances are not that satisfactory. These results indicate that TransRate serves as an excellent transferability predictor for selection of a pre-trained model from various source datasets.

## B.2 Extra Results of Layer Selection

In this subsection, we provide more experiments on the selection of a layer for 14 models pre-trained on different source datasets, including the two experiments presented in Section 4.3. The settings are the same as those in Section 4.3, except that the pre-trained models are trained on different source datasets or with different architectures. Table 4 presents the results of the 14 experiments.

As shown in Table 4, TransRate correctly predicts the performance ranking of transferring different layers in 10 of 14 experiments, where its  $\tau_K$  and  $\tau_\omega$  even equal to 1. In contrast, the best competitor, H-Score, achieves all-correct prediction in only 2 experiments. This shows the superiority of TransRate over the three baseline methods in serving as a criterion for layer selection. In rare cases, H-Score and LogME achieve competitive or even better performances than TransRate, while they fail in most of the experiments. This hit-and-miss behavior can be explained by the assumption behind H-Score and LogME as mentioned in Section 2 – they consider the penultimate layer to be transferred only so that prediction of the transferability at other layers than the penultimate layer is not accurate.

#### B.3 Extra Experiments on Sample Size Sensitivity Study

We provide a supplementary experiment to further investigate the influence of sample size on the performance of transferability estimation algorithms. The performance of an algorithm is evaluated by the Pearson correlation coefficient, Kenddal's  $\tau$  and weighted  $\tau$  on a series of transfer tasks that fine-tune 11 ResNet-18 models pre-trained on different source datsets to Fashion-MNIST. We vary the number of samples per classs in FMNIST from 50 to 6,000, and visulize the trend of the three types of correlation coefficients in Figure 8.

From Fig. 8, we observe that the performance of all algorithms generally drops when the sample size per class decreases from 6,000 to 50. The deterioration of the performance is caused by the inaccurate estimation given a small number of samples. Unlike the baselines, the Kendall's  $\tau$  and weighted  $\tau$  of TransRate drop only by a minor percentage. This shows its superiority in predicting the correct ranking of the models, even when only a small number of samples are available for estimation.

#### B.4 Time complexity

In this subsection, we compare the running time of TransRate as well as the baselines. We run the experiments on a server with 12 Intel Xeon Platinum 8255C 2.50GHz CPU and a single P40 GPU. We consider three

Table 3: Transferability estimation on transferring ResNet-18 pre-trained on 11 different source datasets to different target datasets. The best performance among all transferability measures is highlighted in bold, and the second best is underlined.

Target Datasets	Measures	NCE	LEEP	LFC	H-Score	LogME	TransRate
-	$R_p$	0.4502	0.3697	0.5918	0.5924	0.5785	0.6573
CIFAR-100	$ au_K$	0.2000	-0.0182	0.5272	$\overline{0.7455}$	0.7455	0.6727
	$ au_{\omega}$	0.4813	0.2934	0.7309	0.8394	0.8394	0.7976
	$R_p$	0.4401	0.5416	0.3805	0.6181	0.5792	0.8722
FMNIST	$ au_K$	0.3091	0.0909	0.2727	0.2364	0.1636	0.6363
	$ au_{\omega}$	0.4916	0.3005	0.4828	0.4213	0.3519	0.7892
	$R_p$	-0.7671	-0.3921	-0.6842	0.6885	0.7221	0.7991
Aircraft	$ au_K$	-0.5556	-0.3778	-0.6444	0.6000	0.6000	0.6889
	$ au_{\omega}$	-0.7009	-0.5263	-0.7194	0.6070	0.6070	0.7586
	$R_p$	0.3382	0.5431	0.7222	0.8872	0.8706	0.8419
Birdsnap	$ au_K$	0.1556	0.4222	0.3333	0.6889	0.6889	0.6444
	$ au_{\omega}$	0.3190	0.4987	0.1379	0.5561	0.5561	0.6314
	$R_p$	0.2559	0.5099	0.5817	0.8927	0.8421	0.8655
Caltech-101	$ au_K$	0.1111	0.2444	0.4667	0.8667	0.8667	0.8667
	$ au_{\omega}$	0.4524	0.5404	0.6054	0.9338	0.9338	0.9338
	$R_p$	0.3388	0.5354	0.5373	0.9014	0.8742	0.8892
Caltech-256	$ au_K$	0.2000	0.3333	0.3333	0.8667	0.8667	0.9111
	$ au_{\omega}$	0.4321	0.5298	0.2856	0.7943	0.7943	0.8103
	$R_p$	-0.5717	-0.1674	-0.1548	0.6534	0.6423	0.6941
Cars	$ au_K$	-0.0222	-0.0222	-0.0667	0.2889	0.2889	0.4667
	$ au_{\omega}$	-0.0167	0.0401	0.1040	0.2248	0.1391	0.4330
	$R_p$	-0.2556	-0.2181	0.2744	0.8243	0.7863	0.8271
Flowers	$ au_K$	-0.2889	-0.2444	-0.0222	0.6000	0.6444	0.6444
	$ au_{\omega}$	-0.1258	0.0865	-0.1650	0.5176	0.6035	0.5764
	$R_p$	0.3078	0.4674	0.5332	0.8868	0.8789	0.8826
Food	$ au_K$	0.0222	0.2000	0.2889	0.5556	0.5556	0.6000
	$ au_{\omega}$	0.2089	0.3475	0.1777	0.3688	0.3688	0.4696
	$R_p$	0.3914	0.5012	0.8633	0.9437	0.9158	0.9204
Pets	$ au_K$	0.2889	0.5556	0.9111	0.8667	0.8667	0.8667
	$ au_{\omega}$	0.4730	0.6311	0.9560	0.8141	0.8141	0.9126
	$R_p$	0.1169	0.4184	0.3479	0.9011	0.8884	0.8540
SUN397	$ au_K$	-0.0222	0.2444	0.2444	0.6000	0.6000	0.6000
	$ au_{\omega}$	0.2461	0.4527	0.2427	0.3810	0.3810	0.5579

transfer tasks: 1) transferring ResNet-18 pre-trained on ImageNet to CIFAR-100 with full data; 2) transferring ResNet-18 pre-trained on ImageNet to CIFAR-100 with 1/10 data (50 samples per class); 3) transferring ResNet-50 pre-trained on ImageNet to CIFAR-100 with full data. For task 1), n=50,000, d=512; for task 2), n=5,000, d=512; for task 3), n=50,000, d=2048. The batch size in all experiments is 50.

We present the results in Table 5. First of all, we can observe that the time for fine-tuning a model is about 300 times of the time for transferability estimation (including the time for feature extraction and the time for computing a transferability measure). Besides, it often requires more than 10 times of fine-tuning to search

Table 4: Transferability estimation on transferring different layers of the pre-trained model to the CIFAR-100 dataset. The best performance among all transferability measures is highlighted in bold.

	Measures	LFC	H-Score	LogME	TransRate
Source: SUN397	$R_p$	-0.3108	-0.8636	-0.6370	0.5991
Model: ResNet-18	$ au_K$	0.2000	-0.7333	-0.6000	0.4667
Wiodei. Resivet-16	$ au_{\omega}$	0.1524	-0.8109	-0.6435	0.6625
Source: CIFAR-10	$R_p$	0.6717	0.9668	0.9775	0.9391
Model: ResNet-20	$ au_K$	0.3333	0.8667	0.8667	1.0
Wiodei. Hesivet-20	$ au_{\omega}$	0.3905	0.7551	0.7551	1.0
Source: ImageNet	$R_p$	0.3431	0.9771	0.9914	0.9657
Model: ResNet-18	$ au_K$	0.0	1.0	1.0	1.0
Wiodel. Hesiver-10	$ au_{\omega}$	0.0	1.0	1.0	1.0
Source: ImageNet	$R_p$	0.7100	0.9237	0.9526	0.9375
Model: ResNet-34	$ au_K$	0.2778	0.9444	0.9526	1.0
Wiodei. Resiver-54	$ au_{\omega}$	0.4552	0.8674	0.8674	1.0
Source: Aircraft	$R_p$	0.3512	0.7180	-0.3984	0.8537
Model: ResNet-18	$ au_K$	0.3333	0.6667	-0.3333	1.0
Model. Residet-16	$ au_{\omega}$	0.3333	0.8133	-0.2933	1.0
Source: Birdsnap	$R_p$	0.2602	0.8708	-0.2528	0.8339
Model: ResNet-18	$ au_K$	0.6667	0.6667	-0.3333	0.6667
	$ au_{\omega}$	0.5200	0.8133	-0.2933	0.5200
Source: Caltech-101 Model: ResNet-18	$R_p$	0.8741	0.9213	0.7925	0.9494
	$ au_K$	0.6667	0.6667	0.6667	1.0
	$ au_{\omega}$	0.8133	0.5200	0.5200	1.0
Source: Caltech-256	$R_p$	0.8222	0.8462	-0.6494	0.9379
Model: ResNet-18	$ au_K$	0.6667	0.3333	-0.3333	1.0
Model: ResNet-18	$ au_{\omega}$	0.8133	0.3333	-0.4400	1.0
Source: Cars	$R_p$	-0.6738	0.7091	-0.2494	0.7785
Model: ResNet-18	$ au_K$	-0.3333	0.6667	-0.3333	1.0
Moder. ResNet-16	$ au_{\omega}$	-0.4400	0.8133	-0.3333	1.0
Source: DTD	$R_p$	0.9296	0.8948	0.7231	0.9351
Model: ResNet-18	$ au_K$	1.0	0.6667	0.6667	1.0
Model. Residet-16	$ au_{\omega}$	1.0	0.5200	0.5200	1.0
Source: Flowers	$R_p$	0.8677	0.9196	0.2125	0.9314
Model: ResNet-18	$ au_K$	0.3333	0.6667	0.0	0.6667
Model: ResNet-16	$ au_{\omega}$	0.3333	0.5200	-0.0667	0.5200
Source: Food	$R_p$	0.6372	0.9088	-0.3339	0.9366
Source: Food Model: ResNet-18	$ au_K$	0.6667	1.0	0.3333	0.6667
	$ au_{\omega}$	0.5200	1.0	0.5333	0.5200
Source: Pets	$R_p$	0.7576	0.8985	0.5917	0.9317
Model: ResNet-18	$ au_K$	0.6667	0.6667	0.3333	1.0
wioder Resnet-18	$ au_{\omega}$	0.8133	0.5200	0.2000	1.0
Source: SUN397	$R_p$	0.7168	0.8664	-0.0793	0.9378
	$ au_K$	0.6667	0.3333	0.0	1.0
Model: ResNet-18	$ au_{\omega}$	0.8133	0.3333	-0.0667	1.0

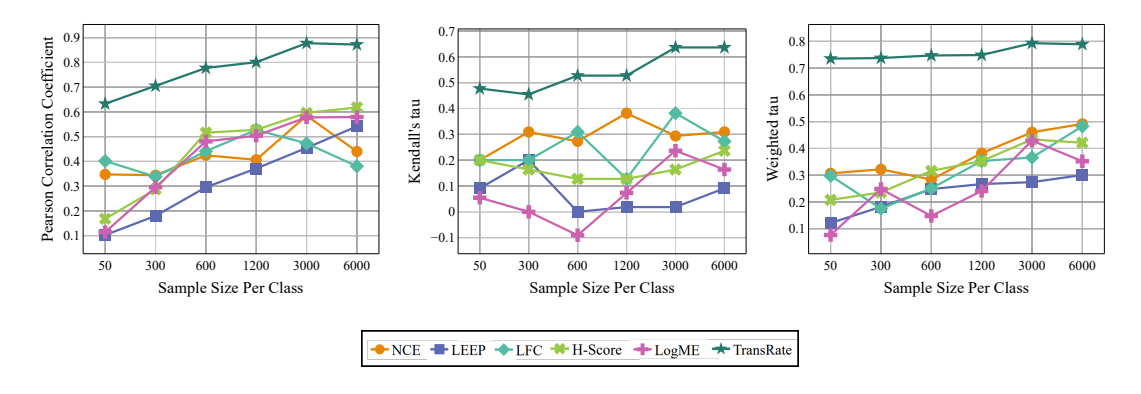


Figure 8: The three types of correlation coefficients between estimated transferability and test accuracy when varying the size of the target dataset (FMNIST in this experiment). The correlation coefficient is measured by a series of transfer tasks that fine-tune the pre-trained ResNet-18 from 11 different source datasets to FMNIST.

for the best-performing hyper-parameters. Therefore, running a transferability estimation algorithm can achieve  $3000\times$  speedup when selecting a pre-trained model and the layer of it to transfer. This highlights the necessity and importance of developing transferability estimation algorithms. Second, though LEEP and NCE computing the similarity between labels only show the highest efficiency, they suffer from the unsatisfactory performance in source selection and the incapability of accommodating unsupervised pre-trained models and layer selection. Third, amongst all the feature-based transferability measures, TransRate takes the shortest wall-clock time. This indicates its computational efficiency. The time costs of both H-Score and LogME are higher than TransRate, which recognizes the necessity of developing an optimization-free estimation algorithm.

## B.5 Sensitivity to Value of $\epsilon$

To evaluate the influence of  $\epsilon$  on the performance of TransRate, we conduct experiments on source selection, layer selection, and model selection with the same settings in Sections 4.2, 4.3, and 4.4, respectively. We vary the value of  $\epsilon^2$  from 0.1 to 10, and report the performance (evaluated by  $R_p$ ,  $\tau$ , and  $\tau_{\omega}$ ) of TransRate under different values of  $\epsilon^2$ .

We have the following three observations. First,  $R_p$  generally decreases as the value of  $\epsilon^2$  increases. For all experiments except the source selection with the target task being FMNIST,  $R_p$  significantly drops when  $\epsilon^2$  changes from 1 to 5. Secondly, the performance evaluated by  $\tau_K$  and  $\tau_\omega$  remains similar when  $\epsilon^2$  is between 0.1 and 5, but significantly decreases when  $\epsilon^2$  changes from 5 to 10. The exception is the experiment of layer selection. In this experiment, the performance significantly degrades when  $\epsilon^2$  increases from 0.5 to 1. Thirdly,

Table 5: Comparison of the computational cost of different measures.

	ResNet-18, Full Data		ResNet-18, Small Γ	Oata	ResNet-50, Full Data		
	Wall-clock time (second)	Speedup	Wall-clock time (second)	Speedup	Wall-clock time (second)	Speedup	
Fine-tune	8399.65	1×	882.33	1×	$2.3 \times 10^{4}$	$1 \times$	
Extract feature	30.1416		3.2986		72.787		
NCE	0.9126	9,204×	0.2119	4,164×	2.1220	10,839×	
LEEP	0.7771	$10,\!808\times$	0.1211	$7{,}286\times$	1.9152	$12,\!009\times$	
LFC	30.1416	279×	0.7987	1,106×	149.3040	154×	
H-Score	1.6285	$5,158 \times$	0.3998	$2,207 \times$	13.07	$1,760 \times$	
LogME	9.2737	$906 \times$	2.0224	$436 \times$	50.1797	$458 \times$	
TransRate	1.3410	$\textbf{6,264} \times$	0.2697	$3,272\times$	10.6498	$2,160\times$	

Table 6: Sensitivity analysis of the value of  $\epsilon$ .

	$  \epsilon^2$	0.1	0.5	1	5	10	
Source Selection Target: CIFAR-100	$ \begin{vmatrix} R_p \\ \tau_K \\ \tau_{\omega} \end{vmatrix} $	0.6573 0.6727 0.7976	0.6465 0.6000 0.7679	0.6200 0.5636 0.7539	$0.5127 \\ 0.5273 \\ 0.7382$	0.4843 $0.4545$ $0.6518$	
Source Selection Target: FMNIST	$ \begin{vmatrix} R_p \\ \tau_K \\ \tau_{\omega} \end{vmatrix} $	0.8722 0.6363 0.7892	0.8324 $0.5872$ $0.7691$	0.8365 $0.5872$ $0.7878$	0.8214 0.6239 0.8078	0.8087 0.5138 0.6936	
Layer Selection	$ \begin{vmatrix} R_p \\ \tau_K \\ \tau_{\omega} \end{vmatrix} $	0.9391 1.0 1.0	0.9325 1.0 1.0	0.9091 0.8667 0.7551	0.8557 $0.8667$ $0.7551$	0.8627 0.8667 0.7551	
Model Selection	$ \begin{vmatrix} R_p \\ \tau_K \\ \tau_{\omega} \end{vmatrix} $	0.9251 0.9048 0.925	0.9211 1.0 1.0	0.9078 $1.0$ $1.0$	0.8366 1.0 1.0	0.7934 $0.9048$ $0.9529$	

Table 7: Transferability estimation on transferring from a pre-trained model to different target tasks.

Target Tasks	Measures	NCE	LEEP	$_{ m LFC}$	H-Score	$\operatorname{LogME}$	${\it TransRate}$
Source: ImageNet	$R_p$	0.9770	0.9696	0.6019	-0.9613	-0.8209	0.8795
Model: ResNet-18	$ au_K$	0.9175	0.9175	0.6674	-0.8137	-0.5448	0.9175
Target: CIFAR-100	$ au_{\omega}$	0.9075	0.9075	0.8095	-0.8546	-0.4774	0.8703
Source: ImageNet	$R_p$	0.8053	0.7910	0.7753	-0.6722	0.6894	0.8175
Model: ResNet-18	$ au_K$	0.6565	0.6659	0.6706	-0.4682	0.6800	0.6753
Target: FMNIST	$ au_{\omega}$	0.7918	0.7885	0.7432	-0.5858	0.7961	0.8380
Source: CIFAR-10	$R_p$	0.9858	0.9865	0.5426	-0.9398	-0.9377	0.9401
Model: ResNet-20	$\tau_K$	0.9058	0.9106	0.5341	-0.8259	-0.7176	0.9294
Target: CIFAR-100	$ au_{\omega}$	0.8780	0.8808	0.6357	-0.8576	-0.7090	0.9141
Source: CIFAR-10	$R_p$	0.7340	0.7412	0.6284	-0.4767	0.7412	0.7748
Model: ResNet-20	$\tau_K$	0.5812	0.5812	0.4400	-0.3506	0.5811	0.6141
Target: FMNIST	$ au_{\omega}$	0.7384	0.7384	0.6320	-0.5448	0.7384	0.7515

we conclude from all the experiments that when  $\epsilon^2$  is small ( $\epsilon^2 < 0.5$ ), its change has limited influence on the performance of TransRate measured by either of the three metrics. Considering  $\epsilon^2 = 0.1$  achieves the best performance in most of the experiments, we set 0.1 as the default value of  $\epsilon^2$  in our experiments.

#### B.6 Target Selection

We follow [12] to also evaluate the correlation of the proposed TransRate and other baselines to the accuracy of transferring a pre-trained model to different target tasks. The target tasks are constructed by sampling different subsets of classes from a target dataset. We consider two target datasets: CIFAR-100 and FMNIST. For CIFAR-100, we construct the target tasks by sampling 2, 5, 10, 25, 50, and 100 classes. For FMNIST, we construct the target tasks by sampling 2, 4, 5, 6, 8, 10 classes. The results on transferring a pre-trained ResNet-18 on Imagenet to two target datasets and transferring a pre-trained ResNet-20 on CIFAR-10 to two target datasets are summarized in Table 7.

The results in Table 7 show that TransRate outshines the baselines in all 4 experiments. In the first experiment, it obtains the same best  $\tau_K$  as NCE and LEEP, although its  $R_p$  and  $\tau_{\omega}$  are a little bit lower than NCE and LEEP. In the second experiment, TransRate achieves the best  $R_p$  and  $\tau_{\omega}$  and the second best  $\tau_K$  (0.6753) which is nearly the same as the best  $\tau_K$  (0.6800). In the third and fourth experiments, TransRate

gets the best  $\tau_K$  and  $\tau_{\omega}$ . Generally speaking, TransRate is the best among all 6 transferability estimation algorithms. Yet we suggest that the competitors, NCE and LEEP, can be good substitutes if TransRate is not considered.

## C Theoretical Details Omitted in Section 3

#### C.1 Proof of Proposition 1.

**Proposition 2.** Assume the target task has a uniform label distribution, i.e.  $p(y = y^c) = \frac{1}{C}$  holds for all c = 1, 2, ..., C. We then have:

$$\operatorname{TrR}_{T_s \to T_t}(g) - H(Y) \gtrsim \mathcal{L}(g, h^*) \gtrsim \operatorname{TrR}_{T_s \to T_t}(g) - H(Y) - H(Z),$$

*Proof.* Firstly, we note that

$$\operatorname{TrR}_{T_s \to T_t}(g) \approx H(Z) - H(Z|Y) = \operatorname{MI}(Y;Z)$$
 (5)

As presented in [53], the mutual information has a variational lower bound as  $MI(Y; Z) \ge \mathbb{E}_{Z,Y} \log \frac{Q(z,y)}{P(z)P(y)}$  for a variational distribution Q. Following [20], we choose Q as

$$Q(z,y) = P(z)P(y)\frac{y \exp(h^*(z))}{\mathbb{E}_{y'}y' \exp(h^*(z))},$$
(6)

where  $h^*(z)$  is the output of optimal classifier before softmax, y is the one-hot label of z, y' is any possible one-hot label. If  $p(y'=y^c)=\frac{1}{C}$  holds for all c=1,2,...,C, we have

$$MI(Y; Z) \geq \mathbb{E}_{Z,Y} \log \frac{y \exp(h^*(z))}{\mathbb{E}_{y'} y' \exp(h^*(z))}$$

$$= \mathbb{E}_{Z,Y} \log \frac{y \exp(h^*(z))}{\frac{1}{C} \sum_{c=1}^{C} y^c \exp(h^*(z))}$$

$$= \mathbb{E}_{Z,Y} \log \frac{y \exp(h^*(z))}{\sum_{c=1}^{C} y^c \exp(h^*(z))} - \log(\frac{1}{C})$$

$$\approx \mathcal{L}(g, h^*) + \log(C)$$

$$= \mathcal{L}(g, h^*) + H(Y)$$

$$(7)$$

The last equality comes from the definition of the negative log-likelihood loss  $\mathcal{L}(g, h^*)$ , which is an empirical estimation of  $\mathbb{E}_{Z,Y} \log \frac{y \exp(h^*(z))}{\sum_{c=1}^C y^c \exp(h^*(z))}$ . Combining Eqs.(5) and (7), we have the first inequality in Proposition

For proving the second inequality, we consider a classifier  $\bar{h}$  that predicts the label y for any data by  $p(y) = \int_{z \in \mathbb{Z}} p(y|z) p(z) dz$ . The the empirical loss computed on this classifier is

$$\mathcal{L}(g,\bar{h}) = \frac{1}{n} \sum_{i=1}^{n} \log p(y_i) = \frac{1}{n} \sum_{i=1}^{n} \log \left( \int_{z \in Z} p(y_i|z) p(z) \right) dz$$

$$\geq \frac{1}{n} \sum_{i=1}^{n} \log p(y_i|z_i) + \frac{1}{n} \sum_{i=1}^{n} \log p(z_i)$$
(8)

The inequality comes from replacing the integral by one of its elements. It is easy to verify that the first term is an empirical estimation of -H(Y|Z) and the second term is an empirical estimation of -H(Z). By the definition of  $\mathcal{L}(g,h^*)$ , we have

$$\mathcal{L}(g, h^*) \ge \mathcal{L}(g, \bar{h}) \gtrsim -H(Y|Z) - H(Z) = \operatorname{TrR}_{T_c \to T_c}(g) - H(Y) - H(Z). \tag{9}$$

Combining Eqns. (7) and (9), we complete the proof.

## C.2 Properties of TransRate Score

In this part, we discuss the properties of the TransRate Score.

**Lemma 1.** For any  $\hat{Z} \in \mathbb{R}^{d \times n}$ , we have

$$R(\hat{Z}, \epsilon) = \frac{1}{2} \log \det(I_d + \frac{d}{n\epsilon^2} \hat{Z} \hat{Z}^\top) = \frac{1}{2} \log \det(I_n + \frac{d}{n\epsilon^2} \hat{Z}^\top \hat{Z})$$

Lemma 1 presents the commutative property of the coding rate, which is known in [16]. Based on this lemma, we can reduce the complexity of  $\log \det(\cdot)$  computation in  $R(\hat{Z}, \epsilon)$  from  $\mathcal{O}(d^{2.373})$  to  $\mathcal{O}(n^{2.373})$  if n < d.

**Lemma 2.** For any  $\hat{Z} \in \mathbb{R}^{d \times n}$  having r singular values, denoted by  $\sigma_1, \sigma_2, ..., \sigma_r$ , we have

$$R(\hat{Z}, \epsilon) = \frac{1}{2} \sum_{i=1}^{r} \log(1 + \frac{d}{n\epsilon^2} \sigma_i^2)$$

Lemma 2 is an inference from the invariant property of the coding rate presented in [16]. Both lemmas are inferred from Sylvester's determinant theorem.

**Lemma 3.** (Upper and lower bounds of TransRate) For any  $\hat{Z}^c \in \mathbb{R}^{d \times n_c}$  for c = 1, 2, ..., C, let  $\hat{Z} = \sum_{c=1}^C \hat{Z}^c$ . We then have

$$\operatorname{TrR}_{T_s \to T_t}(g, \epsilon) = R(\hat{Z}, \epsilon) - \sum_{c=1}^{C} \frac{n_c}{n} R(\hat{Z}^c, \epsilon) \ge 0$$

The equality holds when  $\frac{\hat{Z}\hat{Z}^{\top}}{n} = \frac{\hat{Z}^{c}(\hat{Z}^{c})^{\top}}{n_{c}}$  for all c.

$$\operatorname{TrR}_{T_s \to T_t}(g, \epsilon) = R(\hat{Z}, \epsilon) - \sum_{c=1}^{C} \frac{n_c}{n} R(\hat{Z}^c, \epsilon)$$

$$\leq \frac{1}{2} \sum_{c=1}^{C} \left( \log \det(I_d + \frac{d}{n\epsilon^2} \hat{Z}^c (\hat{Z}^c)^\top) - \frac{n_c}{n} \log \det(I_d + \frac{d}{n_c \epsilon^2} \hat{Z}^c (\hat{Z}^c)^\top) \right)$$

The equality holds when  $\hat{Z}^{c_1}(\hat{Z}^{c_2})^{\top} = 0$  for all  $1 \leq c_1 < c_2 \leq C$ .

The proof follows the upper and lower bound of  $R(\hat{Z}, \epsilon)$  in [54, Lemma A.4].

Remark: Lemma 3 tells that TransRate achieves minimal value when the data covariance matrices of all classes are the same. In this case, it is impossible to separate the data from different classes and no classifier can perform better than random guesses. On the other hand, TransRate achieves its maximal value when the data from different classes are independent. In this case, there exists an optimal classifier that can correctly predict the labels of the data from different classes. The upper and lower bound of TransRate show that TransRate is related to the separability of the data in different classes, and thus, related to the performance of the optimal classifier.

In the end of Section 3.2, we present a toy case of a binary classification problem with  $\hat{Z} = [\hat{Z}^1, \hat{Z}^2]$  where  $\hat{Z}^1 \in \mathbb{R}^{d \times n/2}$  and  $\hat{Z}^2 \in \mathbb{R}^{d \times n/2}$ . The lower and upper bound of the TransRate in this toy case can be derived by Lemma 3. But in Sec. 3.2, we derived the bounds in another way. Here, we provide details of the derivation.

By Lemma 1, we have

$$R(\hat{Z}, \epsilon) = \frac{1}{2} \log \det(I_{2n} + \alpha \hat{Z}^{\top} \hat{Z})$$

$$= \frac{1}{2} \log \det \left( I_n + \alpha \begin{bmatrix} (\hat{Z}^1)^{\top} \hat{Z}^1 & (\hat{Z}^1)^{\top} \hat{Z}^2 \\ (\hat{Z}^2)^{\top} \hat{Z}^1 & (\hat{Z}^2)^{\top} \hat{Z}^2 \end{bmatrix} \right)$$

$$= \frac{1}{2} \log \det \left\{ (I_{n/2} + \alpha (\hat{Z}^1)^{\top} \hat{Z}^1 + \alpha (\hat{Z}^2)^{\top} \hat{Z}^2) + \alpha^2 \left[ (\hat{Z}^1)^{\top} \hat{Z}^1 (\hat{Z}^2)^{\top} \hat{Z}^2 - (\hat{Z}^1)^{\top} \hat{Z}^2 (\hat{Z}^2)^{\top} \hat{Z}^1 \right] \right\}$$

$$\geq \frac{1}{2} \log \det \left\{ (I_{n/2} + \alpha (\hat{Z}^1)^{\top} \hat{Z}^1 + \alpha (\hat{Z}^2)^{\top} \hat{Z}^2) \right\}$$

$$+ \frac{\alpha^2}{2} \log \det \left\{ (\hat{Z}^1)^{\top} \hat{Z}^1 (\hat{Z}^2)^{\top} \hat{Z}^2 - (\hat{Z}^1)^{\top} \hat{Z}^2 (\hat{Z}^2)^{\top} \hat{Z}^1 \right\}$$

$$(10)$$

The first equality comes from Lemma 1; the third equality follows the property of matrix determinant that for any square matrices A, B, C, D with the same size, i.e.,

$$\det\begin{pmatrix} A & B \\ C & D \end{pmatrix} = \det(AD - BC).$$

The inequality follows that for any positive definite symmetric matrices A and B,  $\det(A+B) \geq \det(A) + \det(B)$ . From Eqn (10), we know that when  $(\hat{Z}^1)^\top \hat{Z}^1$  and  $(\hat{Z}^2)^\top \hat{Z}^2$  are fixed, the lower bound of TransRate is related to  $\det \left\{ \left[ (\hat{Z}^1)^\top \hat{Z}^1 (\hat{Z}^2)^\top \hat{Z}^2 - (\hat{Z}^1)^\top \hat{Z}^2 (\hat{Z}^2)^\top \hat{Z}^1 \right] \right\}$ . As the value of this term is determined by  $(\hat{Z}^1)^\top \hat{Z}^2$ , the value of TransRate is also determined by  $(\hat{Z}^1)^\top \hat{Z}^2$ , i.e., the overlap between the two classes. When  $\hat{Z}^1$  and  $\hat{Z}^2$  are completely the same, this term becomes zero and TransRate achieves its minimal value as  $\frac{1}{2} \det \left\{ (I_{n/2} + \alpha(\hat{Z}^1)^\top \hat{Z}^1 + \alpha(\hat{Z}^2)^\top \hat{Z}^2) \right\}$ . When  $\hat{Z}^1$  and  $\hat{Z}^2$  are independent, this term achieves its maximal value as  $\det \left( (\hat{Z}^1)^\top \hat{Z}^1 (\hat{Z}^2)^\top \hat{Z}^2 \right)$  and TransRate achieves its maximal value as well.

#### C.2.1 The Influence of $\epsilon$

In Section 3.2, we mention that the value of  $\epsilon$  has minimal influence on the performance of TransRate. Here we provide more details about the influence of the choice of  $\epsilon$  on the value of TransRate.

Assume that we scale  $\epsilon$  by a positive scaler  $\alpha$ . After scaling, the value of  $R(\hat{Z}, \alpha \epsilon)$  and  $R(\hat{Z}, \alpha \epsilon | Y)$  is different from  $R(\hat{Z}, \epsilon)$  and  $R(\hat{Z}, \epsilon | Y)$ . By Lemma 2, we have

$$R(\hat{Z}, \alpha \epsilon) = \frac{1}{2} \sum_{i=1}^{r} \log(1 + \frac{d}{n\alpha^2 \epsilon^2} \sigma_i^2).$$

If  $\frac{d}{n\alpha^2\epsilon^2}\sigma_i^2\gg 1$ , which holds for a sufficiently small  $\epsilon$ , we have  $\log(1+\frac{d}{n\alpha^2\epsilon^2}\sigma_i^2)\approx\log(\frac{d}{n\alpha^2\epsilon^2}\sigma_i^2)=\log(\frac{d}{n\epsilon^2}\sigma_i^2)-2\log(\alpha)$ . Then for sufficiently small  $\epsilon$ ,  $\alpha$  and sufficiently large  $\sigma_i$ , we have  $R(\hat{Z},\alpha\epsilon)\approx R(\hat{Z},\epsilon)-r\log(\alpha)$  and  $R(\hat{Z},\alpha\epsilon|Y)\approx R(\hat{Z},\epsilon|Y)-r\log(\alpha)$ . Therefore, the influence of  $\alpha$  is nearly canceled in calculating TransRate as we subtract  $R(\hat{Z},\alpha\epsilon)$  by  $R(\hat{Z},\alpha\epsilon|Y)$ . Though this assumption may not hold in practice, we further verify the influence empirically in Appendix B.5.

#### C.3 Time Complexity

When d < n and  $d < n_c$ , the computational costs of  $R(\hat{Z}, \epsilon)$  and  $R(\hat{Z}, \epsilon|Y)$  are  $\mathcal{O}(d^{2.373} + nd^2)$  and  $\mathcal{O}(Cd^{2.373} + Cn_cd^2)$ , respectively. Thus, the total computation cost of TransRate is  $\mathcal{O}((C+1)d^{2.373} + 2nd^2)$ . By Lemma 1, when n < d or  $n_c < d$ , we can further reduce the cost of computing  $R(\hat{Z}, \epsilon)$  or  $R(\hat{Z}, \epsilon|Y)$ . Besides, we can implement the computation of  $R(\hat{Z}, \epsilon)$  and  $R(\hat{Z}^c, \epsilon)$  in parallel, so that we can reduce the computation cost of TransRate to  $\mathcal{O}(\min\{d^{2.373} + nd^2, n^{2.373} + dn^2\})$ .